Interference bunching and antibunching of coherent and atomic radiation fields

P. R. Berman, H. Nguyen, Y. Mei, *Y. Li, and A. Kuzmich Physics Department, University of Michigan, Ann Arbor, Michigan 48109, USA

(Received 10 March 2023; accepted 11 September 2023; published 16 October 2023)

When a coherent field is combined with the phase-matched output of an atomic ensemble, the second-order correlation function of the total field can exhibit superbunching or antibunching. Homodyning the reference field with the atomic emission can amplify the nonclassical characteristics of the atomic emission. A theoretical description of these phenomena is presented. It is pointed out that, even if the number of excitations in the ensemble is much less than unity, truncating a factorized state to have at most two excitations can lead to errors in calculating the second-order correlation function. We also include the effects of dephasing produced by Rydberg-Rydberg interactions and show how they modify the bunching and antibunching that occur in the absence of atom-atom interactions. It is shown that the particle separation probability distribution and the joint particle separation probability distribution play critical roles in determining the effects of dephasing.

DOI: 10.1103/PhysRevA.108.043713

I. INTRODUCTION

In quantum information protocols based on four-wave mixing using Rydberg atoms, there are three stages required to produce an output field radiated by the atoms that has the appropriate quantum properties. First, there is an excitation stage in which pulsed input fields create a coherence between the ground and Rydberg levels in the atoms. Following the excitation stage, there is a storage stage in which there are no input fields present and the atomic dynamics is modified only by atom-atom interactions. Finally, there is a readout stage in which an applied field converts the ground-Rydberg state coherence into a phase-matched output field (PMOF) that is radiated by the atoms. Experimentally, the signals at the detectors are typically integrated over time; as a consequence the dependence of the measured signals on the excitation and storage times is not affected by any dephasing during the readout pulse. Thermal effects are assumed to be negligible.

For this scheme to be useful in quantum information protocols, the interaction energy between excited-state Rydberg atoms must be sufficiently large to produce entanglement between the atoms in the ensemble. For example, in its simplest manifestation, at least in principle, the atom-atom interactions during the excitation phase produce a so-called dipole blockade [1] that results in a single collective Rydberg excitation in the ensemble [2]. Atomic motion can result in decoherence of the collective Rydberg excitation during the storage period, but atom-atom interactions play no significant role since there is only a single Rydberg excitation. A somewhat less efficient way to create a single collective excitation is to produce a multiply excited state in the excitation stage and then allow dipole-dipole interactions to distill that state into a singly excited collective state [3,4]. In both methods, the PMOF is nonclassical, characterized by a time-integrated second-order correlation function $g^{(2)}$ that is less than unity.

If atom-atom interactions can be neglected in both the excitation and storage phases, you might think that the PMOF radiated by an ensemble containing $N \gg 1$ atoms would be second-order coherent, as in conventional theories of four-wave mixing; however, this is true only *approximately*. Without atom-atom interactions, the incident fields create a *factorized* quantum state of the atoms, but a factorized state differs from a coherent state of the atoms [5] by terms of order 1/N. In other words, the factorized atomic state leads to quantum properties in the PMOF, but deviations of $g^{(2)}$ from unity would be very difficult to detect. However, by combining the PMOF with a classical reference field, one can, in effect, amplify the nonclassical aspects of the PMOF.

Interference between a reference field and atomic radiation is most often discussed as the origin of the absorption or gain the reference field experiences in traversing the medium. In other words, the incident field interferes with the scattered radiation in the direction of incidence to diminish or enhance the amplitude of the field. Lampen et al. [6] studied the interference between a weak coherent state reference field and a phase-matched field radiated from either a factorized or single-excitation entangled state. They interpreted their results in terms of Hanbury-Brown correlations between the reference and PMOF. More recently, Wang et al. [7] looked at the interference between a weak coherent state reference field and coherent atomic radiation and the interference between a weak coherent state reference field and radiation from a single collective atomic state. In the case of single collective atomic state radiation, they observed both bunching and antibunching.

In this paper, we show that the value of $g^{(2)}$ associated with the total field that is produced by interfering the PMOF with a classical reference field can be highly nonclassical, exhibiting both extreme bunching ($g^{(2)} \gg 1$) and antibunching ($g^{(2)} \ll 1$), with or without atom-atom interactions. Some general considerations are given in Sec. II. In Sec. III, we neglect atom-atom interactions and assume that the atoms are prepared in a factorized state during the excitation phase.

^{*}Current address: Department of Physics and Astronomy, Washington State University, Pullman, Washington 99164, USA.

Somewhat surprisingly, it is seen that, even if the total number of excitations in the sample is much less than unity, errors can be introduced if the atomic state is truncated to have no more than two excitations. In Sec. IV, we include atom-atom interactions in a truncated atomic state containing at most two excitations. In order to calculate $g^{(2)}$ in this limit, it is necessary to obtain expressions for the particle separation probability density and the joint particle separation probability density (discussed in the Appendix). Two atomic density distributions are considered, a uniform distribution within a sphere of radius R and a spherically symmetric Gaussian distribution. In the limit that all but a single atomic excitation is produced, nonclassical bunching and antibunching can still be observed, resulting from the interference of the PMOF and the classical reference field.

Admittedly some of the features predicted by the theory in Sec. III may be difficult to observe experimentally. Clearly, the signal strength is weak when there is nearly destructive interference in the output. As a consequence, effects such as noise or imperfect overlap of the PMOF and reference fields can make it difficult to observe the superbunching and antibunching. Nevertheless, we have presented these results since we believe them to be of some fundamental interest as well as serving as background to the calculations in Sec. IV.

II. GENERAL CONSIDERATIONS

A rigorous theory of emission would include a detailed analysis that takes into account the temporal and spatial profiles of all the excitation beams, the actual atomic energy level schemes used experimentally, as well as any complications related to modifications of the fields as they propagate through the atomic medium. Instead we adopt a simplified model in which the output field is an independent sum of the PMOF and an input reference field that are combined on a beam splitter. The input reference field is taken to be a multimode (pulsed) coherent state field whose central frequency ω_c matches that of the phase-matched emission. The combined field transmitted into one of the two output ports of the beam splitter is incident on a 50:50 beam splitter and directed towards two detectors, which are equidistant from the beam splitter. Of course, if the combined field exhibits destructive interference in the output port that was chosen, there is constructive interference in the other output port, so as to conserve energy.

The theoretical expression for the PMOF depends on raising and lowering operators associated with the dipole-allowed output transition in the atoms. We assume that these raising and lowering operators are proportional to those of the Rydberg transition at the time the readout pulse is applied [8]. Moreover, we assume perfect spatial and temporal overlap of the PMOF and reference fields. In these limits, the total count \mathcal{P}_1 measured at each detector is proportional to

$$\mathcal{P}_1 \propto 2\epsilon_0 c \langle E(t)E_+(t) \rangle,$$
 (1)

and the total coincidence count \mathcal{P}_2 is proportional to a second-order correlation function $g^{(2)}$ defined by

$$g^{(2)} = \frac{\langle E_{-}(t)E_{-}(t)E_{+}(t)E_{+}(t)\rangle}{\langle E_{-}(t)E_{+}(t)\rangle\langle E_{-}(t)E_{+}(t)\rangle},\tag{2}$$

where $E_+(t) = [E_-(t)]^{\dagger}$ is the positive frequency component of the electric-field operator evaluated at the time t that the

readout pulse is applied. The electric-field operator can be written as a sum of reference and source field operators:

$$E_+ \propto a + B\sqrt{N}S_-,$$
 (3a)

$$E_{-} \propto a^{\dagger} + B\sqrt{N}S_{+},$$
 (3b)

where a (a^{\dagger}) is a destruction (creation) operator for the reference field and S_{\pm} are collective source field operators defined by

$$S_{\pm} = \frac{1}{\sqrt{N}} \sum_{n=1}^{N} \sigma_{\pm}^{(n)}, \tag{4}$$

where $\sigma_{\pm}^{(n)}$ are raising and lowering operators associated with the Rydberg transition in atom n and N is the total number of atoms. The quantity B is a real constant that takes into account the proportionality of the Rydberg raising and lowering operators to those of the transition on which the signal is emitted, as well as a geometrical factor that allows for the fact that only a fraction of the field radiated by the atoms is in the phase-matched direction. The reference field is taken to be classical, allowing us to replace a and a^{\dagger} by the c numbers a and a^{\ast} , respectively, parameters that characterize the strength of the reference field.

It then follows that the (dimensionless) field intensity *I* incident on each detector is proportional to

$$I = \langle (\alpha^* + B\sqrt{N}S_+)(\alpha + B\sqrt{N}S_-) \rangle \tag{5}$$

and the second-order correlation function is given by

$$g^{(2)} = \frac{A}{I^2},\tag{6}$$

where

$$A = \langle (\alpha^* + B\sqrt{N}S_+)(\alpha^* + B\sqrt{N}S_+) \times (\alpha + B\sqrt{N}S_-)(\alpha + B\sqrt{N}S_-) \rangle.$$
 (7)

All the operators appearing in Eqs. (4) and (5) are time-independent Schrödinger operators. The time dependence is contained in the state vector of the atoms, evaluated at the time of application of the readout pulse. All spatial phase factors in the state vector are suppressed in Eqs. (5) and (7) since they will cancel when calculating the field intensity and correlation functions in the phase-matched direction.

We assume that the atoms are excited by a constant amplitude pulsed field having duration T_p and effective Rabi frequency $\Omega=2\chi$ associated with the atom-field coupling of the ground to Rydberg transition. Atom-atom interactions can modify the atom-field dynamics during the excitation phase, as well as the atomic dynamics during the storage phase. Since the readout pulse is always applied after the excitation pulse, we will consider only the signal generated at times $t \geqslant T_P$ in all that follows.

III. NEGLECT OF ATOM-ATOM INTERACTIONS

For sufficiently short excitation and storage times, atomatom interactions can be neglected. In that limit (and with the suppression of spatial phase factors), the state vector for the atoms (in an interaction representation) at any time $t \ge T_P$

following the excitation pulse, but before the readout pulse, can be written as a sum of purely symmetric states:

$$|\psi(t)\rangle = \sum_{n=0}^{N} e^{-in\omega_0 t} \beta_n(T_P) |P_n\rangle, \tag{8}$$

where ω_0 is the ground to Rydberg transition frequency.

$$\sum_{n=0}^{N} |\beta_n(T_P)|^2 = 1,$$
(9)

$$|P_n\rangle = \frac{1}{\sqrt{C_n^N}}|W_n\rangle,\tag{10}$$

 $|W_n\rangle$ is a fully symmetric ket in which n atoms are in their Rydberg states and (N-n) atoms in their ground states, and C_n^N is a binomial coefficient. Without atom-atom interactions, the probability amplitudes β_n are frozen at time $t=T_p$. The $|P_n\rangle$ form an orthonormal basis, $\langle P_n|P_{n'}\rangle = \delta_{n,n'}$, where $\delta_{n,n'}$ is a Kronecker delta. The action of the raising and lowering operators on these symmetric states is given by

$$S_{-}|P_{q}\rangle = \sqrt{q}\sqrt{\frac{N-q+1}{N}}|P_{q-1}\rangle,$$
 (11a)

$$S_{+}|P_{q}\rangle = \sqrt{q+1}\sqrt{\frac{N-q}{N}}|P_{q+1}\rangle.$$
 (11b)

In the limit that $N \gg 1$ and $q \ll N$,

$$S_{-}|P_{q}\rangle \approx \sqrt{q}|P_{q-1}\rangle,$$
 (12a)

$$S_{+}|P_{q}\rangle \approx \sqrt{q+1}|P_{q+1}\rangle,$$
 (12b)

implying that the atomic states can be considered to be coherent states in this limit [5]. For the most part, we will use Eqs. (12) and revert to Eqs. (11) only if $g^{(2)}$ diverges when Eqs. (12) are used. We now evaluate I and $g^{(2)}$ for a factorized atomic state and a truncated atomic state.

A. Factorized state

The state vector for a factorized atomic state is

$$|\psi(t, T_P)\rangle_F = \prod_{n=1}^N [a(T_P)|1\rangle_n + e^{-i\omega_0 t}b(T_P)|2\rangle_n], \qquad (13)$$

where $|1\rangle_n$ is the ket associated with the ground state of atom n and $|2\rangle_n$ is the ket associated with the Rydberg state of atom n. This factorized state is assumed to have been created using coherent radiation fields. By a proper choice of the phases of the atomic state eigenfunctions, it is then possible to have both probability amplitudes $a(T_P)$ and $b(T_P)$ real [9]. In terms of the symmetrized state kets,

$$|\psi(t)\rangle_F = \sum_{n=0}^N e^{-in\omega_0 t} \sqrt{C_n^N} (1-p)^{\frac{N-n}{2}} b^n |P_n\rangle, \qquad (14)$$

where

$$p = b^2 \tag{15}$$

and the T_P dependence of $|\psi\rangle$, b, and p has been suppressed.

Using Eqs. (5), (7), (19), and (11), and defining

$$\alpha_A = BNb\sqrt{1-p},\tag{16}$$

$$f = \frac{\alpha_A}{|\alpha|} = \frac{BNb\sqrt{1-p}}{|\alpha|},\tag{17a}$$

$$\alpha = |\alpha|e^{-i\phi},\tag{17b}$$

we can obtain

$$\frac{I_F}{|\alpha|^2} = 1 + 2f\cos\phi + f^2 + \frac{f^2p}{N(1-p)},\tag{18}$$

and

$$\frac{A_F}{|\alpha|^4} = (1 + 2f\cos\phi + f^2)^2 + \sum_{q=1}^3 \frac{R_q}{N^q},$$
 (19)

where

$$R_1 = \frac{4f^2p - 2f^4(1 - 3p)}{1 - p} - 2f^2\cos(2\phi)$$
$$-\frac{4f^3(1 - 3p)}{1 - p}\cos\phi, \tag{20a}$$

$$R_2 = -\frac{8f^3p}{1-p}\cos\phi + \frac{f^4(1-10p+11p^2)}{(1-p)^2},\quad (20b)$$

$$R_3 = \frac{2f^4p(2-3p)}{(1-p)^2}. (20c)$$

In these expressions, the terms of order N^{-q} reflect the fact that a factorized state differs from a coherent state. We should stress that, although f is proportional to N, it is a free parameter that can be adjusted by varying $|\alpha|$.

If $N \gg 1$,

$$g_F^{(2)} = \frac{A_F}{I_F^2} \tag{21}$$

is approximately equal to unity, unless $\phi = \pi$ and $f \approx 1$. In other words, with the exception of nearly perfect destructive interference, the source field can be considered to be a coherent field. However, if $\phi = \pi$ and f = 1, it follows from Eqs. (18)–(21) that $R_1 = 0$ and

$$g_F^{(2)} = \frac{(1 - 2p + 3p^2)}{p^2} - \frac{2(2 - 3p)}{Np}.$$
 (22)

In this limit $g_F^{(2)} \approx 1/p^2$ if $p \ll 1$. In other words, for a factorized state whose phase-matched emission is out of phase, but equal in amplitude, to the reference field pulse, the value of $g_F^{(2)} \gg 1$ is indicative of the fact that the PMOF radiated by the atoms is nonclassical. In Fig. 1, $g_F^{(2)}$ is plotted as a function of ϕ for f=1, b=0.1, and N=100; a sharp maximum at $\phi=\pi$ is seen. Of course, the fact that $g_F^{(2)} \gg 1$ is linked to the fact that the average intensity at the point of destructive interference is close to zero, that is,

$$I_F(\phi = \pi, f = 1) = \frac{p}{N(1-p)}.$$
 (23)

In practice, noise considerations and phase stability of the reference field will limit the maximum value of $g_F^{(2)}$ that can be observed.

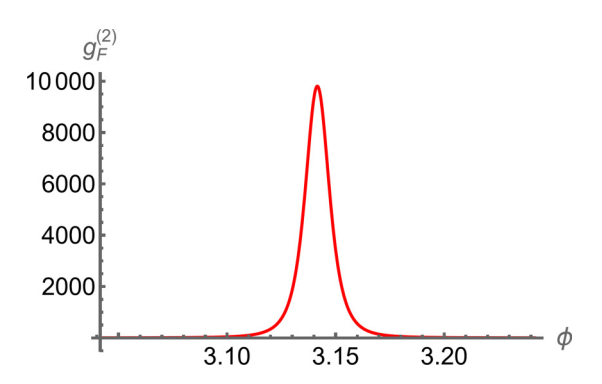


FIG. 1. Second-order correlation function $g_F^{(2)}$ for a factorized state plotted as a function of ϕ for f = 1, b = 0.1, and N = 100.

As f approaches zero, $g_F^{(2)} \approx 1$, consistent with having only the coherent reference field present. On the other hand, as f approaches infinity, and for $N \gg 1$ and $p \ll 1$, $g_F^{(2)} \approx 1 - 2/N$, consistent with having only the atomic field present (see below).

Another interesting feature can be seen in Fig. 2, which is a semilog plot of $g_F^{(2)}$ as a function of f for $\phi=\pi$, b=0.1, and N=100. Aside from the large peak at f=1 there are values of f for which $g_F^{(2)}$ falls below unity. It can be shown that $g_F^{(2)}$ has minima at

$$f_{\pm} \approx 1 + \frac{1 \pm \sqrt{N}}{N - 1} \tag{24}$$

when $N \gg 1$ and $p \ll 1$. Under these conditions, the minimum values achieved are

$$[g_F^{(2)}]_{\pm} \approx 4p \left(1 \mp \frac{2}{\sqrt{N}}\right) \ll 1,$$
 (25)

exhibiting nonclassical behavior. The intensity scales as $1/\sqrt{N}$ at these points, so that noise considerations may limit the amount of antibunching that can be observed.

B. Truncated state

In the absence of atom-atom interactions and for $p \neq 0$, one can never produce a truncated atomic state, as in the dipole blockade. In other words, *all* terms in Eq. (14) con-

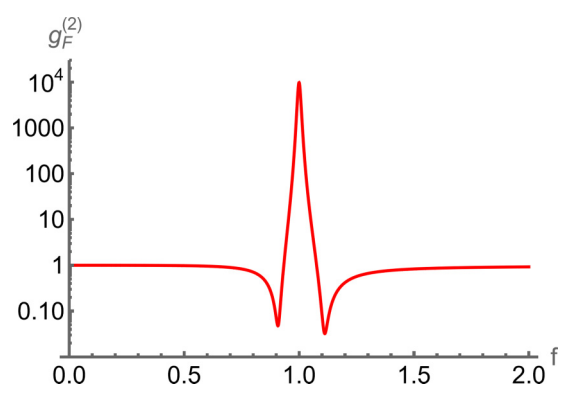


FIG. 2. Semilog plot of the second-order correlation function $g_F^{(2)}$ as a function of f (ratio of atomic to reference field amplitudes) for b = 0.1, $\phi = \pi$, and N = 100.

tribute to the state vector. However, in the limit that the number of excitations in the ensemble is much less than unity, $Np \ll 1$, you might think that a factorized state, truncated to allow for at most two excitations, would provide a good approximation to the exact results for a factorized state. To test this hypothesis, we consider a state having at most two symmetric excitations for which

$$|\psi(t)\rangle_T = \sum_{n=0}^2 e^{-in\omega_0 t} \beta_n |P_n\rangle, \tag{26}$$

with $\beta_n \equiv \beta_n(T_p)$:

$$\sum_{n=0}^{2} |\beta_n|^2 = 1. (27)$$

Eventually the β_n 's (n = 0, 1, 2) will be chosen to match those of a factorized state but, for the moment, we take them to be arbitrary.

When a coherent state pulse α is incident in the phase-matched direction with overlapping pulses, it is not difficult to use Eqs. (5), (7), and (26) to calculate I and A in the limit that $N \gg 1$. The intensity is

$$I_T = |\alpha|^2 + (\alpha^* B \sqrt{N} [\beta_0^* \beta_1 + \sqrt{2} \beta_2 \beta_1^*] + \text{c.c.})$$
$$+ B^2 N [|\beta_1|^2 + 2|\beta_2|^2], \tag{28}$$

and

$$A_{T} = |\alpha|^{4}$$

$$+ 2B|\alpha|^{2} \sqrt{N} \{\alpha^{*} [\beta_{0}^{*} \beta_{1} + \sqrt{2} \beta_{2} \beta_{1}^{*}] + \text{c.c.}\}$$

$$+ 4B^{2} |\alpha|^{2} N[|\beta_{1}|^{2} + 2|\beta_{2}|^{2}]$$

$$+ \sqrt{2}B^{2} N[(\alpha^{*})^{2} \beta_{0}^{*} \beta_{2} + \text{c.c.}]$$

$$+ 2\sqrt{2}B^{3} N^{3/2} [\alpha^{*} \beta_{2} \beta_{1}^{*} + \text{c.c.}] + 2B^{4} N^{2} |\beta_{2}|^{2}. \quad (29)$$

There are essentially four complex parameters that define the reference and atomic fields: α , β_0 , β_1 , and β_2 . Without loss of generalization, we can take β_1 to be real. Defining

$$h = \beta_1 \sqrt{N} B / |\alpha|, \tag{30}$$

$$\alpha = |\alpha|e^{-i\phi},\tag{31a}$$

$$\beta_0 = |\beta_0| e^{i\phi_0},\tag{31b}$$

$$\beta_2 = |\beta_2| e^{i\phi_2},\tag{31c}$$

$$\xi = \frac{2|\beta_2|^2}{\beta_1^4},\tag{31d}$$

$$\Phi = \phi - \phi_0, \tag{31e}$$

$$\Phi' = \phi_0 + \phi_2, \tag{31f}$$

we find

$$g_T^{(2)} = A_T / I_T^2 (32)$$

with

$$\frac{I_T}{|\alpha|^2} = 1 + 2h[|\beta_0|\cos\Phi + \sqrt{\xi}\beta_1^2\cos(\Phi + \Phi')]
+ h^2(1 + \xi\beta_1^2)$$
(33)

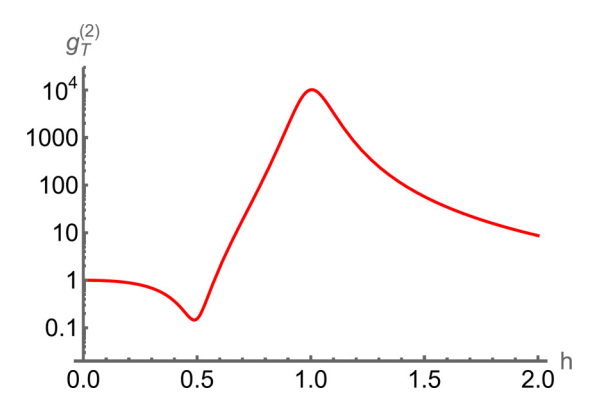


FIG. 3. Semilog plot of the second-order correlation function $g_T^{(2)}$ for a truncated factorized state as a function of h (ratio of atomic to reference field amplitudes) for $\Phi = \pi$, $\beta_1^2 = 0.01$, and $\xi = 0$.

and

$$\frac{A_T}{|\alpha|^4} = 1 + 4h[|\beta_0|\cos\Phi + \sqrt{\xi}\,\beta_1^2\cos(\Phi + \Phi')]
+ 4h^2[1 + \xi\,\beta_1^2] + 2h^2|\beta_0|\sqrt{\xi}\cos(2\Phi + \Phi')
+ 4h^3\sqrt{\xi}\cos(\Phi + \Phi') + h^4\xi,$$
(34)

where

$$|\beta_0| = \sqrt{1 - \beta_1^2 - |\beta_2|^2} = \sqrt{1 - \beta_1^2 - \frac{\xi}{2}\beta_1^4}.$$
 (35)

For $\xi \ll 1$, the fringe visibility is

$$V_{T} \approx \frac{I_{T}(0) - I_{T}(\pi)}{I_{T}(0) + I_{T}(\pi)} \approx \frac{2h[|\beta_{0}| + \sqrt{\xi}\beta_{1}^{2}\cos\Phi']}{1 + h^{2}}$$

$$= \frac{2h[|\beta_{0}| + \sqrt{2}|\beta_{2}|\cos\Phi']}{1 + h^{2}},$$
(36)

which could, in principle, be used to measure Φ' .

An interesting structure appears in $g_T^{(2)} = A_T/I_T^2$ when $\xi \ll 1$ and $\Phi = \pi$, corresponding to almost complete destructive interference if h = 1. In that case,

$$g_T^{(2)} \approx \frac{(1-2h)^2 + 4h(1-\sqrt{1-\beta_1^2})}{\left[(1-h)^2 + 2h(1-\sqrt{1-\beta_1^2})\right]^2}.$$
 (37)

For $\beta_1^2 \ll 1$, $g_T^{(2)} \approx 1/\beta_1^4 \gg 1$ if h=1, while $g_T^{(2)} \approx 16\beta_1^2$ if h=1/2. A semilog plot of $g_T^{(2)}$ as a function of h is shown in Fig. 3 with $\Phi=\pi$, $\beta_1^2=0.01$, and $\xi=0$. This truncated state can exhibit both nonclassical bunching and antibunching. Experimentally, it would be very difficult to see the antibunching since it requires $\beta_1^2 < 1/16$, corresponding to a very low field intensity.

C. The question of whether a factorized state with $Np\ll 1$ reproduces the truncated state result

To answer this question, we take the factorized state values for β_n , namely, $\beta_0 \approx 1 - Np/2$, $\beta_1 = \sqrt{Np}$, and $\beta_2 \approx Np/\sqrt{2}$ ($\xi \approx 1$, $\Phi' = 0$, $h = f/\sqrt{1-p}$). Although Eq. (27) is not strictly satisfied with these values, it is satisfied approximately when $Np \ll 1$. As can be seen in the semilog plots

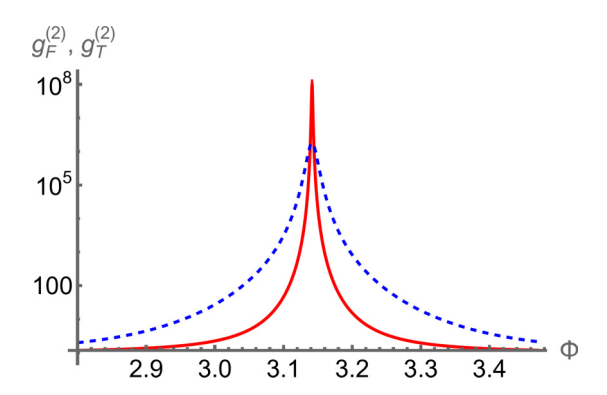


FIG. 4. Semilog plots of the second-order correlation functions for a factorized state (solid red curve) and a truncated factorized state (dashed blue curve) as a function of Φ . Despite the fact that the average number of excitations in the ensemble is 0.01, the two results do not agree.

of Fig. 4, where $g_T^{(2)}$ and $g_F^{(2)}$ are plotted as a function of Φ for f=1,N=100, $p=b^2=0.0001,$ $\xi=1,$ and $\Phi'=0,$ the two results do not agree at all near $\Phi=\pi$. If $Np\ll 1$, it follows from Eq. (22) that $g_F^{(2)}(f=1,\Phi=\pi)\approx 1/p^2,$ whereas, from Eqs. (32)–(35), one can show that

$$g_T^{(2)}(f=1, \Phi=\pi) \approx \frac{1}{p^2} \left[\frac{1+pN^3}{1+pN^3 + \frac{(pN^3)^2}{4}} \right],$$
 (38)

which differs from $1/p^2$ if $pN^3 \gtrsim 1$. In addition, in contrast to the results plotted in Fig. 2, $g_T^{(2)}$ does not exhibit a sharp dip near f=0.9 when plotted as a function of f for N=100, p=0.0001, and $\Phi=\pi$, as shown in Fig. 5. How can this be explained? It turns out that the condition $Np \ll 1$ is necessary, but not sufficient, for the two results to agree. The reason for this is a bit subtle, however. In our calculations, we take $h=\beta_1\sqrt{N}B/|\alpha|=NBb/|\alpha|$ to be a free parameter; that is, no matter how small b is, we can choose $|\alpha|$ in such a manner to get any value of h we wish. In other words, even though $h^n \propto b^n$, h^n need not be a small quantity. As a consequence, higher-order terms in the truncated state are needed

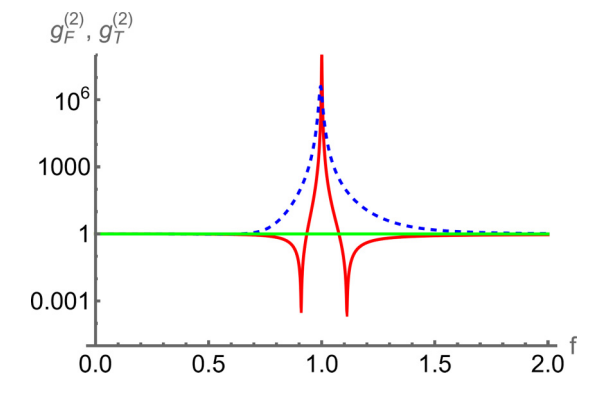


FIG. 5. Semilog plots of the second-order correlation functions for a factorized state (solid red curve) and a truncated factorized state (dashed blue curve) as a function of f. Despite the fact that the average number of excitations in the ensemble is 0.01, the two results do not agree.

to reproduce the factorized state result. We have verified that, for a truncated state formed by truncating a factorized state, $g_T^{(2)} = g_F^{(2)}$ to order p^2 when $Np \ll 1$, provided the sum in Eq. (14) is truncated at n = 4 rather than n = 2.

IV. INCLUSION OF ATOM-ATOM INTERACTIONS

Atom-atom interactions modify the field radiated by the atoms. In a previous paper, we analyzed the role of dephasing on the atomic emission in the limit that dephasing is important in the storage stage but could be neglected during the excitation stage [4]. It was assumed in that paper that the excitation pulse produced a factorized state having $n \ge 2$ excitations and that dephasing reduced the ground-Rydberg coherence during the storage phase. Even with that assumption, the calculation was relatively simple only for n = 2, when the intensity and $g^{(2)}$ depend only on the particle separation probability density and the joint particle separation probability density. Each higher value of n introduces yet a new multiparticle separation probability density. The extension of the theory to allow for dephasing effects in the excitation phase is by no means trivial if there are more than two excitations. As a consequence, and to illustrate the physics, we limit the discussion to truncated states containing at most two excitations for which the field intensity and the correlation function depend only on the single and joint particle separation probability distributions. We have seen already that, in the absence of atom-atom interactions and in the perturbation theory limit, truncating a factorized state to have at most two excitations leads to errors in calculating the correlation function. To avoid this problem, we assume that dephasing plays a non-negligible result in the excitation phase. In this limit, dephasing can convert the factorized state that would be produced if there were no Rydberg-Rydberg interactions into a truncated state containing at most two excitations. We neglect all corrections of order 1/N.

Let us denote the probability of n excitations in the ensemble by E_n . We are interested in the limit that $E_2 \ll E_1$ and assume that the incident field(s) creates at most two excitations in an ensemble of N atoms. We take as the state vector in an interaction representation

$$|\psi(t)\rangle_{2} = c_{0}(t)|g\rangle + \sum_{n=1}^{N} c_{n}(t)e^{-i\omega_{0}t}|n\rangle$$

$$+ \sum_{\substack{n,n'=1\\n'>n}}^{N} c_{nn'}(t)e^{-2i\omega_{0}t}|nn'\rangle, \tag{39}$$

where $|g\rangle$ is the ket with all atoms in state 1, $|n\rangle$ is the ket with atom n in state 2 and all other atoms in state 1, and $|nn'\rangle$ is the ket with atoms n and n' in state 2 and all other atoms in state 1. We neglect all spatial phase factors since they will not contribute in the phase-matched direction. The initial condition is that the ensemble is in the ground state before the fields are applied.

In the presence of dephasing, the limit of at most two excitations can be achieved in two ways. If the driving field is sufficiently weak to ensure that

$$\sqrt{N}A \ll 1,$$
 (40)

where A is the pulse area, then the average number of excitations in the ensemble is much less than unity. We refer to this as the perturbation theory limit. Alternatively, for a maximum effective Rabi frequency Ω of the field(s) and a characteristic Rydberg-Rydberg interaction shift Δ that satisfy

$$\frac{\sqrt{N}\Omega}{|\Delta|} \ll 1,\tag{41}$$

the blockade limit is realized in which the number of double excitations is much less than unity. If neither of these inequalities hold, it is necessary to include terms beyond the doubly excited states.

If $E_2 \ll E_1$, all the $c_n(t) = c_1(t)$ are equal and we can define

$$C_1(t) = \frac{1}{\sqrt{N}} \sum_{n=1}^{N} c_n(t) = \sqrt{N} c_1(t), \tag{42}$$

such that

$$|\psi_{2}(t)\rangle = C_{0}(t)|P_{0}\rangle + C_{1}(t)e^{-i\omega_{0}t}|P_{1}\rangle$$

$$+ e^{-2i\omega_{0}t} \sum_{\substack{n,n'=1\\n'>n}}^{N} c_{nn'}(t)|nn'\rangle. \tag{43}$$

A. Calculation of I_2 and $g_2^{(2)}$

First let us calculate the intensity:

$$I_2 = |\alpha|^2 + \sqrt{N}B(\alpha^*\langle S_-\rangle + \text{c.c.}) + NB^2\langle S_+S_-\rangle. \tag{44}$$

Using Eqs. (12) and (43), we find

$$\langle S_{-} \rangle = C_1 C_0^* + \frac{C_1^*}{N} K,$$
 (45a)

$$\langle S_{+}S_{-}\rangle = |C_{1}|^{2} + \frac{F}{N}, \tag{45b}$$

and

$$\frac{I_2}{|\alpha|^2} = 1 + h \left(\frac{C_1 C_0^* \alpha^*}{|C_1||\alpha|} + \text{c.c.} \right) + h^2
+ \frac{h}{N} \left(\frac{C_1^* \alpha^* K}{|C_1||\alpha|} + \text{c.c.} \right) + \frac{h^2}{N|C_1|^2} F,$$
(46)

where

$$h = \frac{\sqrt{NB|C_1|}}{|\alpha|},\tag{47a}$$

$$K = \sum_{\substack{n,n'=1\\n' \neq n}}^{N} c_{nn'}, \tag{47b}$$

$$F = \sum_{n=1}^{N} \left| \sum_{n' \neq n=1}^{N} c_{nn'} \right|^{2}.$$
 (47c)

We next must calculate

$$A_{2} = |\alpha|^{4} + 2|\alpha|^{2} \sqrt{N} B(\alpha^{*} \langle (S_{-}) \rangle + \text{c.c.}) + 4|\alpha|^{2} N B^{2} \langle S_{+} S_{-} \rangle + N B^{2} ((\alpha^{*})^{2} \langle S_{-}^{2} \rangle + \text{c.c.}) + 2 N^{3/2} B^{3} (\alpha^{*} \langle S_{+} S_{-}^{2} \rangle + \text{c.c.}) + N^{2} B^{4} \langle S_{+} S_{+} S_{-} S_{-} \rangle.$$
(48)

With

$$\langle S_{-}^{2} \rangle = C_{0}^{*} K, \tag{49}$$

$$\langle S_+ S_-^2 \rangle = C_1^* K, \tag{50}$$

$$\langle S_+ S_+ S_- S_- \rangle = |K|^2, \tag{51}$$

we find

$$\frac{A_2}{|\alpha|^4} = 1 + 2h \left(\frac{C_1 C_0^* \alpha^*}{|C_1| |\alpha|} + \text{c.c.} \right) + 4h^2 \left(1 + \frac{F}{N|C_1|^2} \right)
+ \frac{2h}{N} \left(\frac{C_1^* \alpha^*}{|C_1| |\alpha|} K + \text{c.c.} \right)
+ \frac{h^2}{N|C_1|^2} \left(C_0^* \frac{(\alpha^*)^2}{|\alpha|^2} K + \text{c.c.} \right)
+ 2 \frac{h^3}{N|C_1|^2} \left(\frac{C_1^* \alpha^* K}{|C_1| |\alpha|} + \text{c.c.} \right)
+ \frac{h^4}{N^2 |C_1|^4} |K|^2.$$
(52)

B. Evaluation of $g_2^{(2)}$

To evaluate $g_2^{(2)} = A_2/I_2^2$, we need values of $C_1 = \sqrt{N}c_1$, C_0 , and $c_{nn'}$. We take as our Hamiltonian in an interaction representation

$$H = \hbar \chi \sum_{n=1}^{N} (\sigma_{+}^{(n)} + \sigma_{-}^{(n)}) + \sum_{\substack{n,n'=1\\n'>n}}^{N} \hbar \Delta_{nn'} \sigma_{2}^{(n)} \sigma_{2}^{(n')}$$
 (53)

where χ is one half of the effective Rabi frequency associated with the Rydberg transition, $\Delta_{nn'}$ is a Rydberg-Rydberg interaction shift that is assumed to be a function only of

$$R_{nn'} = |\mathbf{R}_n - \mathbf{R}_{n'}|,\tag{54}$$

 \mathbf{R}_n is the position of atom n, and $\sigma_2^{(n)}$ is the Rydberg state population operator of atom n. The first term in the Hamiltonian represents the resonant driving of the Rydberg transition by an effective field [10]. The second term in Eq. (53) characterizes the dipole-dipole or van der Waals interaction that gives rise to excitation-induced dephasing and is responsible for the dipole blockade. We shall take

$$\Delta_{nn'} = C_{\text{Rvd}} / R_{nn'}^6. \tag{55}$$

With this Hamiltonian, and in the limit that the probability to have two excitations is much less than $|C_1(t)|^2$, the equations of motion for the state amplitudes are given approximately by

$$\dot{c}_0 = -\chi \Theta(t)\Theta(T_p - t) \sum_{n=1}^{N} c_n, \tag{56a}$$

$$\dot{c}_n = \chi \Theta(t) \Theta(T_p - t) c_0, \tag{56b}$$

$$\dot{c}_{nn'} = \chi \Theta(t)\Theta(T_p - t)(c_n + c_{n'}) - i\Delta_{nn'}c_{nn'}, \quad (56c)$$

where Θ is a Heaviside function and we have chosen the wave-function phases such that $\chi = i|\chi|$. Dephasing affects only the $c_{nn'}$ amplitudes since it is necessary to have two excitations if Rydberg-Rydberg interactions are to play a role.

1. Perturbation theory

In perturbation theory, to ensure that $C_0 \approx 1$, it is necessary that the inequality given in Eq. (40) is satisfied. In this limit, for $t \geqslant T_p$,

$$C_0 \approx 1 - \frac{|C_1|^2}{2} = 1 - \frac{N\chi^2 T_p^2}{2},$$
 (57a)

$$c_n(t) = \frac{C_1}{\sqrt{N}} \approx \chi T_p, \tag{57b}$$

$$c_{nn'}(t) \approx 2\chi^{2} \int_{0}^{T_{p}} t' e^{-i\Delta_{nn''}(t-t')} dt'$$

$$= \frac{2\chi^{2}}{\Delta_{nn'}^{2}} [e^{-i\Delta_{nn'}(t-T_{p})} (1 - i\Delta_{nn'}T_{p}) - e^{-i\Delta_{nn'}t}].$$
(57c)

With $\alpha = |\alpha|e^{-i\phi}$,

$$K \to K_{\text{PT}} = \sum_{\substack{n,n'=1\\n' \to n}}^{N} c_{nn'} = N^2 \chi^2 T_p^2 Q_{\text{PT}},$$
 (58)

$$F \to F_{\text{PT}} = \sum_{n=1}^{N} \left| \sum_{n' \neq n=1}^{N} c_{nn'} \right|^2 \approx N^3 \chi^4 T_p^4 G_{\text{PT}},$$
 (59)

and

$$h = \frac{\sqrt{N}B|C_1|}{|\alpha|} = \frac{N\chi T_p}{|\alpha|},\tag{60}$$

it then follows from Eqs. (46), (57), (55), (47b), and (47c) that

$$\frac{I_{\text{2PT}}}{|\alpha|^2} \approx 1 + 2h\cos\phi + h^2 + \epsilon[-h\cos\phi + h(Q_{\text{PT}}e^{i\phi} + \text{c.c.}) + h^2G_{\text{PT}}], \quad (61)$$

where

$$Q_{\rm PT}(\tau_p, \tau) = \int ds P(s) f_{\rm PT}(s, \tau_p, \tau), \tag{62a}$$

$$G_{\text{PT}}(\tau_p, \tau) = \int ds \int ds' P(s, s') f_{\text{PT}}(s, \tau_p, \tau) f_{\text{PT}}^*(s', \tau_p, \tau),$$
(62b)

$$f_{\text{PT}}(s, \tau_p, \tau) = 2 \frac{e^{-i(\tau - \tau_p)/s^6} (1 - i\tau_p/s^6) - e^{-i\tau/s^6}}{\tau_p^2/s^{12}}, \quad (63)$$

$$\epsilon = C_1^2 = N\chi^2 T_p^2 \ll 1, \quad (64)$$

 τ and τ_p are dimensionless variables that are defined below, and (see the Appendix) P(s) is the (dimensionless) particle separation probability distribution and P(s,s') is the (dimensionless) joint particle separation probability distribution. In writing Eqs. (62), we have gone over to continuous variables by replacing the sums in Eqs. (47b) and (47c) by integrals over the volume of the sample. As was noted previously, the intensity depends on both P(s) and P(s,s').

When $\phi = \pi$ and h = 1,

$$\frac{I_{\text{2PT}}(\phi = \pi, h = 1)}{|\alpha|^2} \approx \epsilon (1 - 2 \operatorname{Re} Q_{\text{PT}} + G_{\text{PT}}). \tag{65}$$

This equation is valid only for times when Q_{PT} and G_{PT} deviate from unity by at least terms of order ϵ ; that is, they cannot be used in the limit of no interactions, when $Q_{PT} \approx 1$ and $G_{PT} \approx 1$. In that limit, $I_{2PT}(\phi = \pi, h = 1) \approx 0$, a result that is not consistent with Eq. (33) for h = 1, $\phi = \pi, \xi = 1$, and $\Phi' = 0$, since we have implicitly neglected all corrections of order ϵ^2 in this section in deriving Eq. (65).

We consider two density distributions: a uniform distribution $W_{un}(\mathbf{r})$ within a sphere having a radius equal to R,

$$W_{\rm un}(\mathbf{r}) = \frac{1}{(4\pi R^3/3)}\Theta(R-r),$$
 (66)

and a spherical Gaussian distribution:

$$W_G(\mathbf{r}) = \sqrt{\frac{1}{\pi a^3}} e^{-r^2/a^2}.$$
 (67)

For the uniform distribution, the (dimensionless) particle separation probability distribution (see the Appendix) is

$$P_{\rm un}(s) = \left(3s^2 - \frac{9}{4}s^3 + \frac{3}{16}s^5\right)\Theta(2-s),\tag{68}$$

where s = r/R. For the spherical Gaussian distribution, it is

$$P_G(s) = \sqrt{\frac{2}{\pi}} s^2 e^{-s^2/2},\tag{69}$$

where s = r/a. A program such as MATHEMATICA can be used to obtain long analytic expressions for $Q_{\rm PT}$ using Eqs. (62a), (68), and (69), expressed as a function of dimensionless times defined by

$$\tau_p(x) = C_{\text{Rvd}} T_p / x^6, \tag{70a}$$

$$\tau(x) = C_{\text{Rvd}} t / x^6, \tag{70b}$$

where x = R for the uniform distribution and x = a for the spherical Gaussian distribution.

The situation is somewhat different for the joint particle separation distribution P(s, s'). In the Appendix, it is shown that

$$P_G(s, s') = \frac{8}{\pi\sqrt{3}}ss'\sinh\left(\frac{2ss'}{3}\right)\exp\left(-\frac{2}{3}(s^2 + s'^2)\right),$$
 (71)

but we have not been able to obtain the corresponding analytic expression for a spherical uniform distribution. For both distributions, the function $G_{\rm PT}$ must be calculated numerically. It turns out that errors of less than 10% are produced for most of the range of the distribution if one approximates

$$P(s, s') \approx P(s')P(s).$$
 (72)

In this limit, it follows from Eqs. (62) that $G_{\text{PT}}(\tau_p, \tau) = |Q_{\text{PT}}(\tau_p, \tau)|^2$. To check the validity of this approximation, in Fig. 6 we plot $G_{\text{PT}}(\tau, \tau)$ (solid green curve), $|Q_{\text{PT}}(\tau, \tau)|^2$ (dashed blue curve), $G_{\text{PT}}(10, \tau)$ (solid red curve), and $|Q_{\text{PT}}(10, \tau)|^2$ (dashed brown curve) as a function of τ for a spherical Gaussian distribution. The curves $G_{\text{PT}}(\tau, \tau)$ and $|Q_{\text{PT}}(\tau, \tau)|^2$ characterize the role of dephasing in the excitation stage $(\tau = \tau_p)$ and the curves $G_{\text{PT}}(10, \tau)$ and $|Q_{\text{PT}}(10, \tau)|^2$ characterize the role of dephasing in the storage stage. The results are qualitatively the same for a uniform distribution, as shown in Fig. 7. The solid curves in Fig. 7 were

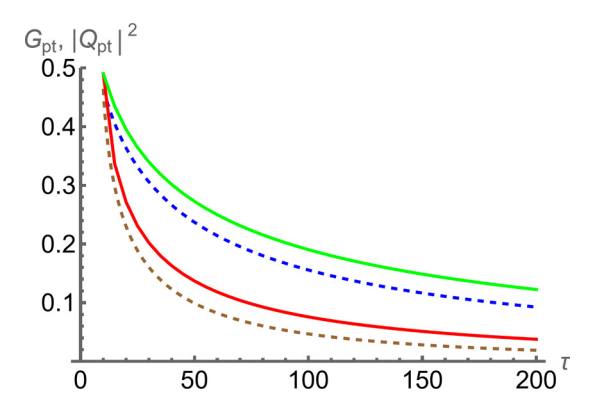


FIG. 6. Graphs of $G_{\rm PT}(\tau,\tau)$ (upper, solid green curve), $|Q_{\rm PT}(\tau,\tau)|^2$ (upper, dashed blue curve), $G_{\rm PT}(10,\tau)$ (lower, solid red curve), and $|Q_{\rm PT}(10,\tau)|^2$ (lower, dashed brown curve) plotted as a function of τ for a spherical Gaussian distribution.

calculated directly from Eqs. (59) and (57c) using a Monte Carlo simulation.

We now turn our attention to A_2 . Using Eqs. (52), (47), (64), and (57), we find

$$\frac{A_{2PT}}{|\alpha|^4} = 1 + 4h\left(1 - \frac{\epsilon}{2}\right)\cos\phi + 4h^2
+ 2\epsilon[h(Q_{PT}e^{i\phi} + \text{c.c.}) + h^2G_{PT}]
+ h^2(e^{2i\phi}Q_{PT} + \text{c.c.}) + 2h^3(e^{i\phi}Q_{PT} + \text{c.c.})
+ h^4|Q_{PT}|^2.$$
(73)

We should like to stress again that these equations are valid only for times τ_p when $Q_{\rm PT}$ and $G_{\rm PT}$ deviate from unity by at least terms of order ϵ , that is, when $(1-|Q_{\rm PT}|)/\epsilon\gg 1$, $(1-G_{\rm PT})/\epsilon\gg 1$. Otherwise higher-order terms need to be kept to ensure that Eqs. (61) and (73) agree with Eqs. (18) and (19), respectively.

We are interested in the value of the correlation function $g_{\rm 2PT}^{(2)}(\tau_p,\tau)=A_{\rm 2PT}(\tau_p,\tau)/I_{\rm 2PT}(\tau_p,\tau)^2$ as a function of both τ and τ_p . For $\tau_p\gg 1$ or $(\tau-\tau_p)\gg 1$, both $G_{\rm PT}(\tau_1,\tau)$ and

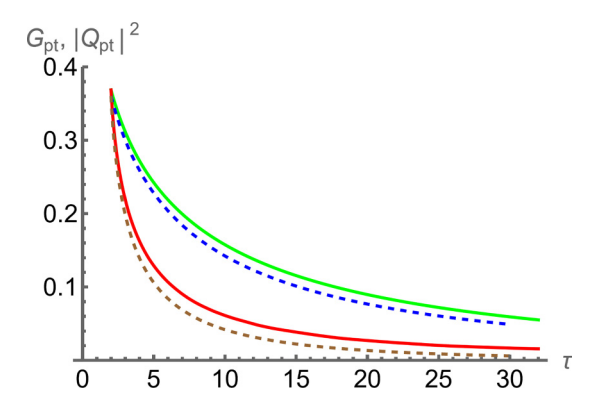


FIG. 7. Graphs of $G_{\rm PT}(\tau,\tau)$ (upper, solid green curve), $|Q_{\rm PT}(\tau,\tau)|^2$ (upper, dashed blue curve), $G_{\rm PT}(2,\tau)$ (lower, solid red curve), and $|Q_{\rm PT}(2,\tau)|^2$ (lower, dashed brown curve) plotted as a function of τ for a uniform distribution.

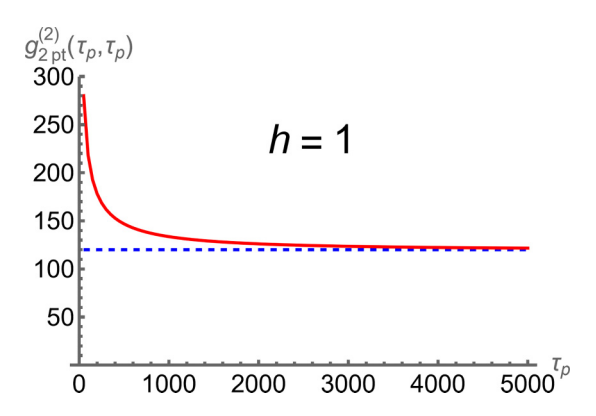


FIG. 8. Second-order correlation function $g_{\rm 2PT}^{(2)}(\tau_p,\tau_p)$ for a spherical Gaussian atomic density distribution as a function of τ_p for $\{h=1,\epsilon=0.1,\phi=\pi\}$. The dashed blue line is the asymptotic limit when $Q_{\rm PT}\approx 0$ and $G_{\rm PT}\approx 0$.

 $Q_{\rm PT}(\tau_1,\tau)$ go to zero and

$$g_{\text{2PT}}^{(2)} \approx \frac{1 + 4h(1 - \frac{\epsilon}{2})\cos\phi + 4h^2}{\left[1 + 2h(1 - \frac{\epsilon}{2})\cos\phi + h^2\right]^2}.$$
 (74)

It is clear from this expression that $g_2^{(2)}$ can exhibit non-classical behavior if h=1 (superbunching) or $h\approx 1/2$ (antibunching) for $\phi=\pi$. In Figs. 8 and 9, we plot $g_{2\text{PT}}^{(2)}(\tau_p,\tau_p)$ for a spherical Gaussian atomic density distribution as a function of τ_p for $\{h=1,\epsilon=0.1\}$ (superbunching) or $\{h=1/2,\epsilon=0.01\}$ (antibunching) for $\phi=\pi$. These curves show that dephasing during the excitation phase dramatically reduces the value of $g_2^{(2)}(\tau_p,\tau_p)$ from its interaction-free value. For $\tau>\tau_p$, dephasing further reduces the value of $g_2^{(2)}(\tau_p,\tau)$ by damping the emission from the doubly excited atomic states, ultimately reaching the asymptotic limit given by Eq. (74). In contrast to the case of atomic radiation only studied in Ref. [4], dephasing in the storage period does not necessarily lead to $g_2^{(2)} \ll 1$, since the one-photon component of the atomic field can still interfere with the reference field. However, for $h\gg 1$, $\epsilon\ll 1$, and $\phi=\pi$, $g_2^{(2)}\approx 4(1+3/h)/h^2\ll 1$. A plot of $g_2^{(2)}(50,\tau)$ for a spherical Gaussian distribution as a function of $\tau>50$ is shown in Fig. 10 for h=10 and $\epsilon=0.1$. It is seen that $g_2^{(2)}(\tau_p,\tau)$ exhibits something like

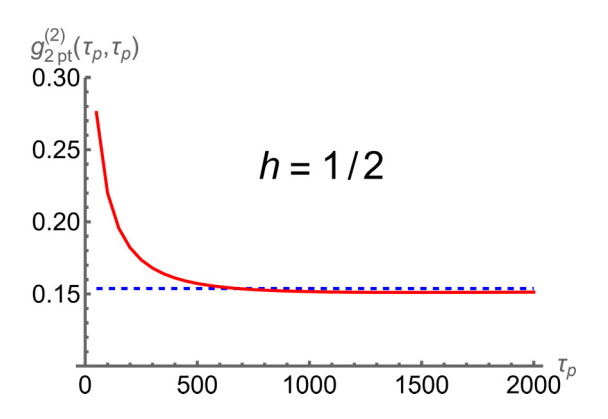


FIG. 9. Second-order correlation function $g_{\rm 2PT}^{(2)}(\tau_p,\tau_p)$ for a spherical Gaussian atomic density distribution as a function of τ_p for $\{h=1/2,\epsilon=0.01,\phi=\pi\}$. The dashed blue line is the asymptotic limit when $Q_{\rm PT}\approx 0$ and $G_{\rm PT}\approx 0$.

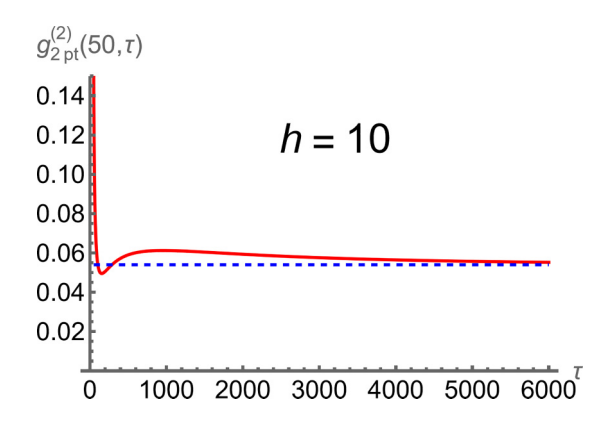


FIG. 10. Second-order correlation function $g_{2\text{PT}}^{(2)}(50, \tau_p)$ for a spherical Gaussian atomic density distribution as a function of τ for $\{h=10, \epsilon=0.1, \phi=\pi\}$. The dashed blue line is the asymptotic limit when $Q_{\text{PT}}\approx 0$ and $G_{\text{PT}}\approx 0$.

overdamped behavior. The results are similar for a uniform distribution, except that the overdamped behavior is more pronounced. This is seen in Figs.11 and 12, where $g_2^{(2)}(10,\tau)$ is plotted for a uniform distribution as a function of $\tau > 10$, h = 10, and $\epsilon = 0.1$. The signal exhibits damped periodic motion with period $\approx 2\pi \times 64$ in approaching the asymptotic limit [Eq. (74)] shown by the dashed line.

2. Dipole blockade limit

The second case for which an analytic approximation is valid is when

$$\sqrt{N} \left| \frac{\chi}{\Delta_{nn'}} \right| \ll 1, \tag{75}$$

allowing us to treat $c_{nn'}$ in perturbation theory. In this limit, for $t \ge T_p$,

$$c_0 \approx \cos(\sqrt{N}\chi T_p) = C_0, \tag{76a}$$

$$c_n \approx \frac{\sin(\sqrt{N}\chi T_p)}{\sqrt{N}} = \frac{C_1}{\sqrt{N}},$$
 (76b)

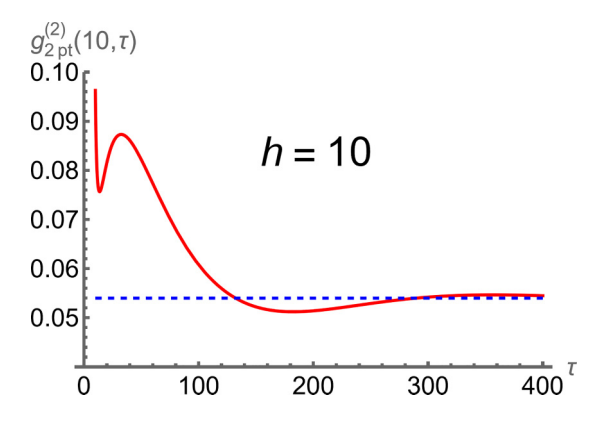


FIG. 11. Second-order correlation function $g_{\rm 2PT}^{(2)}(10, \tau_p)$ for a uniform atomic density distribution as a function of τ for $\{h=10, \epsilon=0.1, \phi=\pi\}$. The dashed blue line is the asymptotic limit when $Q_{\rm PT}\approx 0$ and $G_{\rm PT}\approx 0$.

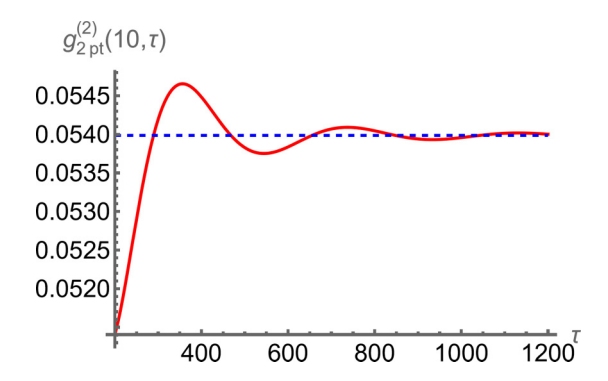


FIG. 12. Same as Fig. 11, showing the damped oscillations.

$$c_{nn'} \approx -\frac{2\chi}{i\Delta_{nn'}} e^{-i\Delta_{nn'}(t-T_p)} c_n$$

$$= 2i\chi \frac{\sin(\sqrt{N}\chi T_p)}{\sqrt{N}\Delta_{nn'}} e^{-i\Delta_{nn'}(t-T_p)}.$$
(76c)

Dephasing produces a nearly perfect blockade in the excitation stage and the small, doubly excited component is further reduced by dephasing in the storage stage.

With

$$K \to K_{\text{DB}} = \sum_{\substack{n,n'=1\\n'\neq n}}^{N} \tilde{c}_{nn'} \sim iN\epsilon(x)\sin(\sqrt{N}\chi T_p)Q_{\text{DB}}, \quad (77)$$
$$F \to F_{\text{DB}} = \sum_{n=1}^{N} \left| \sum_{n'\neq n=1}^{N} \tilde{c}_{nn'} \right|^{2}$$
$$\sim N\epsilon^{2}(x)\sin^{2}(\sqrt{N}\chi T_{p})G_{\text{DB}}, \quad (78)$$

we find the intensity

$$\begin{split} \frac{I_{\text{2DB}}}{|\alpha|^2} &= 1 + 2h\cos(\sqrt{N}\chi T_p)\cos\phi + h^2 \\ &+ h\epsilon\sin(\sqrt{N}\chi T_p)(ie^{i\phi}Q_{\text{DB}} + \text{c.c.}) \\ &+ h^2\epsilon^2G_{\text{DB}} \end{split} \tag{79}$$

where

$$h = \frac{\sqrt{N}B\sin(\sqrt{N}\chi T_p)}{|\alpha|},$$

$$Q_{\mathrm{DB}}(\tau_{p}, \tau) = \int ds P(s) f_{\mathrm{DB}}(s, \tau_{p}, \tau), \tag{80a}$$

$$G_{\mathrm{DB}}(\tau_{p}, \tau) = \int ds \int ds' P(s, s') f_{\mathrm{DB}}(s, \tau_{p}, \tau) \times f_{\mathrm{DB}}^{*}(s', \tau_{p}, \tau), \tag{80b}$$

$$f_{\rm DB}(s, \tau_p, \tau) = s^6 e^{-i(\tau - \tau_p)/s^6},$$
 (81)

$$\epsilon(x) = \frac{2\sqrt{N}\chi}{C_{\text{Rvd}}/x^6},\tag{82}$$

and x = R for the uniform distribution and x = a for the spherical Gaussian distribution. For $\tau = \tau_p$, $Q_{\rm DB} = 64/15$ and $G_{\rm DB} = 1769\,984/75\,075$ for the uniform distribution and $Q_{\rm DB} = 106$ and $G_{\rm DB} = 123\,795/4$ for the spherical Gaussian distribution. Recall that the blockade limit is valid only for $\epsilon \ll 1$.

Similarly, we find

$$\frac{A_{2\text{DB}}}{|\alpha|^4} = 1 + 4h\cos(\sqrt{N}\chi T_p)\cos\phi + 4h^2
+ h\epsilon\sin(\sqrt{N}\chi T_p)(ie^{i\phi}Q_{\text{DB}} + \text{c.c.})
+ 4h^2\epsilon^2G_{\text{DB}}
+ h^2\frac{\epsilon\cos(\sqrt{N}\chi T_p)}{\sin(\sqrt{N}\chi T_p)}(ie^{2i\phi}Q_{\text{DB}} + \text{c.c.})
+ 2h^3\frac{\epsilon}{\sin(\sqrt{N}\chi T_p)}(ie^{i\phi}Q_{\text{DB}} + \text{c.c.})
+ h^4\left[\frac{\epsilon}{\sin(\sqrt{N}\chi T_p)}\right]^2|Q_{\text{DB}}|^2.$$
(83)

If $\epsilon \ll 1$, then, to a good approximation,

$$g_{\text{2DB}}^{(2)} \approx \frac{1 + 4h\cos(\sqrt{N}\chi T_p)\cos\phi + 4h^2}{(1 + 2h\cos(\sqrt{N}\chi T_p)\cos\phi + h^2)^2}.$$

If $\sqrt{N}\chi T_p = 2n\pi + \delta$ where $\epsilon \ll \delta \ll 1$, and $\phi = \pi$, or if $\sqrt{N}\chi T_p = (2n+1)\pi + \delta$ and $\phi = 0$, it is possible to have large $g_{\text{2DB}}^{(2)}$ for h = 1 and small $g_{\text{2DB}}^{(2)}$ for h = 1/2. Dephasing no longer plays a significant role since the probability of having two excitations is small and, in contrast to the perturbative limit, the probability of having two excitations is independent of the probability for having a single excitation.

V. DISCUSSION

When a coherent field is mixed with the phase-matched output of an atomic ensemble, interesting features can appear in the second-order correlation function. We have seen that, even though the fields separately lead to a second-order correlation function that is approximately equal to unity, the combined fields can exhibit superbunching or antibunching. In effect, heterodyning the reference field with the atomic emission can amplify the nonclassical characteristics of the atomic emission. In other words, for an ensemble containing $N \gg 1$ atoms, the phase-matched radiation has a secondorder correlation function that is approximately equal to unity. However, when mixed with a coherent reference field, the combined fields can exhibit nonclassical properties, related to the fact that a factorized atomic state is not a coherent state. Corrections of order 1/N become important when there is close to total destructive interference of the two fields.

The role of Rydberg-Rydberg interactions has also been examined. It was shown that, when there are at most two

excitations in the ensemble, the effect of dephasing can be related to two quantities: the particle separation probability distribution and the joint particle separation probability distribution. The particle separation probability distribution has been calculated for a uniform atomic density distribution and a spherical Gaussian density distribution. Moreover an analytic expression was obtained for the joint particle separation probability distribution for the spherical Gaussian density distribution. Dephasing tends to diminish the superbunching, but can actually lead to enhanced antibunching.

ACKNOWLEDGMENT

This research is funded by NSF and AFOSR.

APPENDIX

When at most two excitations are included, two types of integrals enter when dephasing is included, corresponding to the functions Q and G of the text defined by Eqs. (58), (59), (77), and (78). The sums over n are replaced by integrals using the prescription

$$\sum_{n=1}^{N} \to N \int d\mathbf{s} W(\mathbf{s}),$$

where $W(\mathbf{s})$ is the (dimensionless) distribution function for the particles. In terms of dimensionless variables, it is then possible to write Q as

$$Q = \int d\mathbf{s}_1 \int d\mathbf{s}_2 W(\mathbf{s}_1) W(\mathbf{s}_2) f(s), \tag{A1}$$

where

$$\mathbf{s} = \mathbf{s}_2 - \mathbf{s}_1,\tag{A2}$$

and $f(s = |\mathbf{s}_2 - \mathbf{s}_1|)$ is a function that depends on the atomfield interaction. We define the particle separation probability distribution P(s) by

$$Q = \int ds P(s) f(s). \tag{A3}$$

Similarly we can write G as

$$G = \int d\mathbf{s}_1 \int d\mathbf{s}_2 \int d\mathbf{s}_3 W(\mathbf{s}_1) W(\mathbf{s}_2) W(\mathbf{s}_3) f(s) f^*(s'),$$
(A4)

where

$$\mathbf{s}' = \mathbf{s}_3 - \mathbf{s}_1. \tag{A5}$$

We define the joint particle separation probability distribution P(s, s') by

$$G = \int ds \int ds' P(s, s') f(s) f^*(s'). \tag{A6}$$

1. $P_{un}(s)$ and $P_{un}(s, s')$ for a uniform distribution

Here we present a relatively simple derivation of Eq. (68). We use dimensionless variables \mathbf{s} for displacement vectors and, in terms of these variables, the sphere radius is equal to 1. Without loss of generalization, we can take \mathbf{s} along the -z direction. The formal equation for P(s), obtained using

Eqs. (A1)–(A3), is

$$P_{\rm un}(s) = s^2 \int d\Omega_s \int d\mathbf{s}_1 W(\mathbf{s}_1) W(\mathbf{s}_1 + \mathbf{s}). \tag{A7}$$

For a uniform spherical particle distribution,

$$W(\mathbf{s}_1) = 1/(4\pi/3)\Theta(1 - s_1),$$
 (A8)

where Θ is a Heaviside function. In this case,

$$P_{\text{un}}(s) = \frac{9s^2}{4\pi} \int_0^1 s_1^2 ds_1 \int_0^1 \sin \theta_1 d\theta_1 \int_0^1 d\phi_1 \Theta(1 - |\mathbf{s}_1 + \mathbf{s}|)$$

$$= \frac{9s^2}{2} \int_0^1 s_1^2 ds_1 \int_0^1 \sin \theta_1 d\theta_1$$

$$\times \Theta[1 - (s_1^2 + s^2 - 2ss_1 \cos \theta_1)]. \tag{A9}$$

The Heaviside function vanishes unless $s \le 2$. The integral can now be evaluated separately for s > 1 and s < 1.

If s > 1, the Heaviside function vanishes unless $s_1 > s - 1$ and

$$\cos \theta_1 < \frac{s_1^2 + s^2 - 1}{2ss_1},\tag{A10}$$

such that

$$P_{\rm un}(s) = \frac{9s^2}{2}\Theta(2-s)\int_{s-1}^1 s_1^2 ds_1 \int_0^{\cos^{-1}\left(\frac{s_1^2+s^2-1}{2ss_1}\right)} \sin\theta_1 d\theta_1$$
$$= \left(3s^2 - \frac{9}{4}s^3 + \frac{3}{16}s^5\right)\Theta(2-s). \tag{A11}$$

For s < 1, we must consider two limits, $s + s_1 < 1$ and $s + s_1 > 1$ For $s + s_1 < 1$, any θ_1 is allowed and $s_1 < 1 - s$, but for $s + s_1 > 1$, Eq. (A10) must hold and $s_1 > 1 - s$. Thus,

$$P_{\text{un}}(s) = \frac{9s^2}{2}\Theta(2-s) \int_0^{1-s} s_1^2 ds_1 \int_0^{\pi} \sin\theta_1 d\theta_1$$

$$+ \frac{9s^2}{2}\Theta(2-s) \int_{1-s}^1 s_1^2 ds_1 \int_0^{\cos^{-1} \left(\frac{s_1^2 + s^2 - 1}{2ss_1}\right)\pi} \sin\theta_1 d\theta_1$$

$$= \left(3s^2 - \frac{9}{4}s^3 + \frac{3}{16}s^5\right)\Theta(2-s), \tag{A12}$$

yielding the same result as for s > 1 [11].

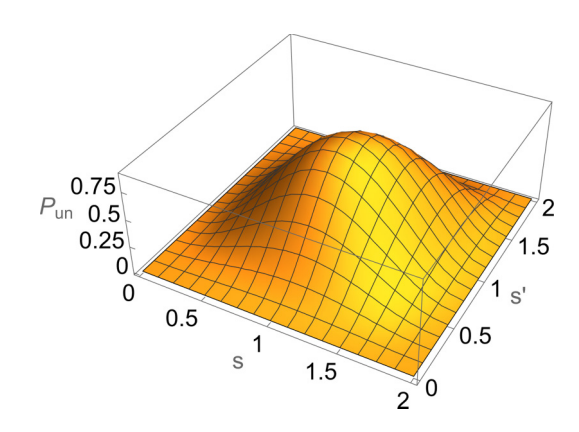


FIG. 13. Graph of the joint probability distribution for a uniform atomic density distribution.

The corresponding expression for $P_{un}(s, s')$, obtained using Eqs. (A4)–(A6) with s taken along the -z axis and s' in the x-z plane at an angle θ' to the z axis, is then

$$P_{\text{un}}(s, s') = \frac{27}{8\pi} s^2 s'^2 \int_0^1 s_1^2 ds_1 \int_0^{\pi} \sin \theta_1 d\theta_1$$

$$\times \int_0^{2\pi} d\phi_1 \int_0^{\pi} \sin \theta' d\theta'$$

$$\times \Theta \left[1 - \left(s_1^2 + s^2 - 2ss_1 \cos \theta_1 \right) \right]$$

$$\times \Theta \left[1 - \left(s_1^2 + s'^2 + 2ss' \cos \beta \right) \right], \quad (A13)$$

where

$$\cos \beta = \cos \theta_1 \cos \theta' + \sin \theta_1 \sin \theta' \cos \phi_1. \tag{A14}$$

We have not been able to obtain an analytic expression for $P_{\rm un}(s,s')$ for this uniform distribution, but the results using numerical integration are shown in Fig. 13.

2. $P_G(s)$ and $P_G(s, s')$ for a spherical Gaussian distribution

For a dimensionless spherical Gaussian distribution,

$$W(\mathbf{s}) = \frac{1}{\pi^{3/2}} e^{-s^2}.$$
 (A15)

It is now a simple matter to calculate

$$P_G(s) = s^2 \int d\Omega_s \int d\mathbf{s}_1 W(\mathbf{s}_1) W(\mathbf{s}_1 + \mathbf{s})$$
$$= \sqrt{\frac{2}{\pi}} s^2 e^{-\frac{s^2}{2}}.$$
 (A16)

For the spherical Gaussian distribution, one can also get an analytic expression for the joint particle separation distribution, obtained from Eqs. (A4)–(A6) as

$$P_G(s, s') = s^2 s'^2 \int d\Omega_s \int d\Omega_{s'}$$

$$\times \int d\mathbf{s}_1 W(\mathbf{s}_1) W(\mathbf{s}_1 + \mathbf{s}) W(\mathbf{s}_1 + \mathbf{s}'). \quad (A17)$$

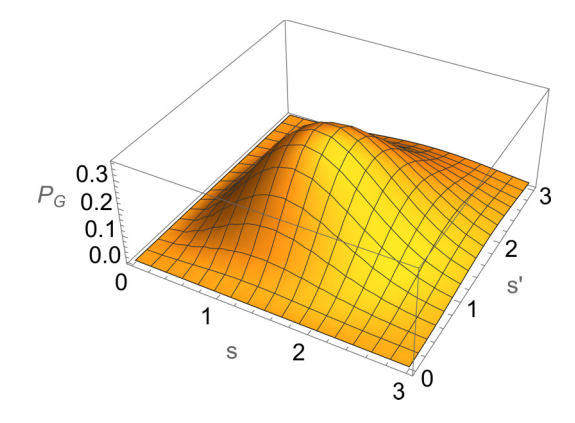


FIG. 14. Graph of the joint probability distribution for a spherical Gaussian atomic density distribution.

To start, we write this as

$$P_G(s, s') = \left(\frac{1}{\sqrt{\pi}}\right)^9 s^2 s'^2 \int d\Omega_s \int d\Omega_{s'}$$

$$\times \exp\left[-3\left(\mathbf{s}_1 + \frac{2(\mathbf{s} + \mathbf{s}')}{3}\right)^2\right]$$

$$-\left[s^2 + s'^2 + (\mathbf{s} + \mathbf{s}')^2/3\right]$$

$$= \left(\frac{1}{\sqrt{\pi}}\right)^6 \left(\frac{1}{\sqrt{3}}\right)^3 \int d\Omega_s \int d\Omega_{s'}$$

$$\times \exp\left[-\frac{2}{3}(s^2 + s'^2 + \mathbf{s} \cdot \mathbf{s}')\right]. \tag{A18}$$

To proceed further, we expand

$$\exp\left[-\frac{2}{3}\mathbf{s}\cdot\mathbf{s}'\right]$$

$$= 4\pi \sum_{\ell=0}^{\infty} \sum_{m=-\ell}^{\ell} i^{\ell} Y_{\ell m}(\theta,\phi) Y_{\ell m}^{*}(\theta',\phi') j_{\ell}\left(-i\frac{2ss'}{3}\right),$$
(A19)

where j_{ℓ} is a spherical Bessel function. The integrals over angles then yield $4\pi \delta_{\ell,0} \delta_{m,0}$ and

$$P_G(s, s') = \frac{16}{\pi} \left(\frac{1}{\sqrt{3}}\right)^3 s^2 s'^2 \exp\left(-\frac{2}{3}(s^2 + s'^2)\right) j_0\left(-i\frac{2ss'}{3}\right)$$
$$= \frac{8}{\pi\sqrt{3}} ss' \sinh\left(\frac{2ss'}{3}\right) \exp\left(-\frac{2}{3}(s^2 + s'^2)\right). \tag{A20}$$

A graph is shown in Fig. 14.

- M. D. Lukin, M. Fleischhauer, R. Cote, L. M. Duan, D. Jaksch, J. I. Cirac, and P. Zoller, Phys. Rev. Lett. 87, 037901 (2001); for reviews of this subject, see D. Comparat and P. Pillet, J. Opt. Soc. Am. B 27, A208 (2010); M. Saffman and T. G. Walker, Rev. Mod. Phys. 82, 2313 (2010); A. Browaeys and T. Lahaye, Nat. Phys. 16, 132 (2020).
- [2] Y. O. Dudin and A. Kuzmich, Science 336, 887 (2012); Y. O. Dudin, L. Li, F. Bariani, and A. Kuzmich, Nat. Phys. 8, 790 (2012); Y. Mei, Y. Li, H. Nguyen, P. R. Berman, and A. Kuzmich, Phys. Rev. Lett. 128, 123601 (2022).
- [3] F. Bariani, Y. O. Dudin, T. A. B. Kennedy, and A. Kuzmich, Phys. Rev. Lett. 108, 030501 (2012); F. Bariani, Paul M.

- Goldbart, and T. A. B. Kennedy, Phys. Rev. A **86**, 041802(R) (2012).
- [4] Y. Li, Y. Mei, H. Nguyen, P. R. Berman, and A. Kuzmich, Phys. Rev. A 106, L051701 (2022).
- [5] F. T. Arecchi, E. Courtens, R. Gilmore, and H. Thomas, Phys. Rev. A 6, 2211 (1972).
- [6] J. Lampen, A. Duspayev, H. Nguyen, H. Tamura, P. R. Berman, and A. Kuzmich, Phys. Rev. Lett. 123, 203603 (2019).
- [7] X. Wang, J. Wang, Z. Ren, R. Wen, C.-L. Zou, G. A. Siviloglou, and J. F. Chen, Phys. Rev. Lett. 128, 083605 (2022).
- [8] P. R. Berman and A. Kuzmich, Phys. Rev. A 101, 033824 (2020).
- [9] In general, a factorized state of the form $|\psi\rangle_F = \prod_{n=1}^N (a_n|1\rangle_n + e^{-i\omega_0 t}b_n|2\rangle_n)$ is *not* a fully symmetric state unless all the a_n 's are equal and all the b_n 's are equal. In writing Eq. (13), we
- have neglected any propagation effects for the excitation field and assumed that it creates the same superposition state for each atom (aside from a spatial phase factor which has been suppressed). In this case, the relative phase between a and b depends only on id, where d is the dipole moment operator matrix element between states $|1\rangle$ and $|2\rangle$. By a proper choice of the phases of the eigenfunctions, both a and b will be real.
- [10] In most cases the ground-to-Rydberg transition is a two-photon transition driven by two fields However, by adiabatically eliminating the intermediate state in this two-photon transition, one arrives at an effective Rabi frequency for the transition.
- [11] The particle separation distribution for a uniform spherical density has been calculated by a number of authors. See, for example, S.-J. Tu and E. Fischbach, arXiv:math-ph/0004021 (2000), and references therein; M. Perry and E. Fischbach, J. Math. Phys. 41, 2417 (2000), and references therein.